The Journal of Experimental Biology 208, 1905-1913
Published by The Company of Biologists 2005
doi:10.1242/jeb.01573

Contractile properties of mouse single muscle fibers, a comparison with amphibian muscle fibers

K. A. P. Edman

Department of Physiological Sciences, Biomedical Centre, F11, University of Lund, S-221 84 Lund, Sweden

e-mail: paul.edman@farm.lu.se

Accepted 7 March 2005

Summary

Single fibers, 25–40 μm wide and 0.5–0.7 mm long, were isolated from the flexor digitorum brevis muscle of the mouse. Force and movement were recorded (21–27°C) from the fiber as a whole and, in certain experiments, from a short marked segment that was held at constant length by feedback control. The maximum tetanic force, 368±57 kN/m^2 (*N*=10), was not significantly different from that recorded in frog muscle fibers at equal temperature. However, the rising phase of the tetanus was considerably slower in the mammalian fibers, 202±20 ms (*N*=17) being required to reach 90% of maximum tetanic force as compared with 59±4 ms (*N*=20) in the frog muscle fibers. Similar to the situation in frog muscle fibers, the force–velocity relation exhibited two distinct curvatures located on either side of a breakpoint near 80% of the isometric force. Maximum speed of shortening was 4.0±0.3 fiber lengths s^{-1} (*N*=6). The relationship between tetanic force and sarcomere length was studied between 1.5 and 4.0 μm sarcomere spacings, based on length-clamp recordings that were free of 'tension creep'. There was a flat maximum (plateau) of the length-tension relation between approximately 2.0 and 2.4 μm sarcomere lengths. The descending limb of the length-tension relation (linear regression) intersected the length axis (zero force) at 3.88 μm and reached maximum force at 2.40 μm sarcomere length. The slope of the descending limb is compatible with a thick filament length of 1.63 μm and an average thin filament length of 1.10 μm. These values accord well with recent electron microscope measurements of myofilament length in mammalian muscle.

Key words: muscle fiber, muscle contraction, mammalian muscle, force–velocity relationship, length–tension relationship.

Introduction

Our present knowledge of muscle mechanics is in large part gained from studies of isolated frog muscle, as amphibian muscles show extraordinary stability over long experiments and are suitable for isolation of intact single fibers. The latter aspect is of particular relevance as it enables the study of various contraction parameters – such as force, instantaneous stiffness and shortening velocity – under the strict control of sarcomere length, within a selected region of the fiber (e.g. Ford et al., 1977; Edman and Reggiani, 1984; Piazzesi et al., 2002). Similar studies on mammalian muscle have been hampered by the difficulties in isolating intact single fibers from these muscles to enable mechanical measurements of the kind previously performed in amphibian fibers. Thus, there is still a lack of information in mammalian muscle concerning the time course of force development during twitch and tetanus under conditions where filament sliding is restrained by feedback control of the sarcomere length. Nor have the force–velocity–length relationships been accessible for a detailed analysis like that described in studies of amphibian muscle. Although the structural arrangement of the sarcomeres, the transverse tubules and the sarcoplasmic reticulum is similar in amphibian and mammalian muscles, it still remains to be established to what extent the functional properties of the two muscle species accord with one another at single fiber level.

The present investigation has been performed on isolated mouse muscle fibers using techniques that previously have been employed in studies of amphibian fibers. Interest has been focussed on the shape of the force–velocity relationship, as previous studies of frog muscle fibers have shown that the force–velocity relation in these muscles is not a simple hyperbolic function, as originally thought (Hill, 1938), but contains two distinct portions on either side of a breakpoint in the high-force range (Edman, 1988). This observation suggests that the kinetics of cross-bridge function is changed as the load on the muscle exceeds a critical value (Edman et al., 1997). With the techniques used it has furthermore been possible to length clamp a limited region of an isolated mammalian muscle fiber, in this way making it feasible to delineate the relationship between force and sarcomere length in the preparation used.

Materials and methods

Preparation and mounting of muscle fibres

The experiments were performed according to procedures

approved by the Animals Ethics Committee of the University of Lund. Single fibers were dissected from the flexor digitorum brevis muscle of the hindlimb of the mouse (NMRI, weight 25–30 g). The dissection was carried out by means of a fine pair of scissors, and care was taken to avoid undue stretching of the fibers during the dissection procedure. Only fibers that had an insignificant amount of connective tissue were selected for this study. The fibers, approximately 25–40 μm wide and 0.5–0.7 mm in length between the tendon insertions, were mounted horizontally in a thermostatically controlled Perspex chamber, between a force transducer and an arm extending from the moving coil of an electromagnetic puller. For mounting the fiber, small clips of aluminium foil, similar to those illustrated in fig. 1 of Edman and Reggiani (1984), were affixed to each tendon and attached to a small hook of stainless-steel wire on the tip of the tension transducer and the puller arm. The side parts of the aluminium clips were folded tightly around the hooks to prevent any change in the position of the clip during the experiment. By adjusting the angle at which the clips were attached to the steel hooks, it was possible to minimize any lateral, vertical or twisting movements of the muscle fiber during isometric contraction. During the experiment, a glass coverslip (0.1 mm thickness) was placed on top of the muscle chamber between the force transducer and the puller arm. In addition to providing a plane upper surface, the presence of the coverslip ensured that the bath temperature remained constant with no gradients along the length of the preparation (to within ±0.1°C) during the experiment. This latter point was tested by using a thermistor probe that was moved underneath the coverslip by means of a micromanipulator.

The flexor digitorum brevis muscle (FDB) of the mouse is classified as a ‘fast’ skeletal muscle. A recent study (González et al., 2003) based on immunostaining techniques has demonstrated that fibers expressing the fast-type myosin heavy chain (MHC) isoforms IIX and IIA were predominant in FDB, amounting to 83–87% of the fiber population. No staining for the fast-type MHC IIB was observed. An additional 13–17% of the fibres expressed the slow-type MHC I. A similar isomyosin composition of the FDB of the mouse has been observed by Reggiani and co-workers (C. Reggiani, personal communication), based on gel electrophoretical separation. However, in the latter study, myosin isoform IIB was constantly found to be present in approximately 10% of the fibre population.

Solutions

The bathing solution had the following composition (mmol l^{-1}): NaCl, 137; KCl, 5; $MgCl_2$, 1; NaH_2PO_4, 1; $NaHCO_3$, 16; Glucose, 11; $CaCl_2$, 2; pH 7.4. The bathing solution was equilibrated with a mixture of 95% O_2 and 5% CO_2 before entering the muscle chamber, the latter being thermostatically controlled by circulating a water-glycerol solution from a Colora Ultrathermostat (Colora Messtechnik GMBH, Lorch, Germany) through jackets surrounding the muscle chamber. The bathing fluid was perfused through the muscle chamber (volume, approximately 2.5 ml) at a speed of approximately 2 ml min^{-1}. The bath temperature was constant to within 0.2°C during any given experiment, but varied between 21 and 27°C among the different experiments. Fiber length and fiber width were determined as described by Edman and Reggiani (1984). Contrary to the relatively thick frog muscle fibers, whose cross-section is markedly irregular in shape from one end to the other (see Blinks, 1965), the thinner mouse fibers were found to have a more uniform, rounded shape. The cross-section of the mouse muscle fibers was therefore calculated from the measured fiber diameter (d) assuming a circular cross-section, i.e. as $\pi\ (d/2)^2$.

Determination of sarcomere length

Because the thin, single muscle fibers gave a very weak laser diffraction pattern, the sarcomere length was measured at rest at 800× magnification within a marked segment of the fiber. This was achieved at a given length of the segment by means of a light microscope that was fitted with a 40× water-immersion objective and an ocular micrometer. Rows of about 20 sarcomeres were measured and a mean value of the sarcomere length was formed. By knowing the sarcomere length at rest, the overall sarcomere spacing within the segment could be determined at any time during activity by monitoring the length of the marked segment (see below). Unless otherwise stated, the experiments were performed at a resting sarcomere length of 2.6–2.7 μm, i.e. just above slack fiber length.

Force transducer

The principal unit of the force transducer was a semiconductor strain-gauge element (AE 801, Aksjeselskapet Mikroelektronikk, Horten, Norway). A thin extension (approximately 5 mm in length) made of wood was glued by epoxy resin to the silicon bar outside the domain of the strain-gauge elements. The tip of the extended arm was provided with a hook of stainless-steel wire (diameter, 0.1 mm) for attachment of the muscle fiber (see above). The resonant frequency was approximately 2 kHz when the transducer arm was submerged in the bathing solution.

Stimulation

Rectangular pulses of 0.2 ms duration were passed between a pair of platinum plate electrodes that were placed symmetrically, approximately 4 mm apart, on either side of the muscle fiber. The stimulus strength was set to approximately 15% above the mechanical threshold. A train of pulses of appropriate frequency (60–80 Hz) was used to produce a fused tetanus of 0.5–1 s duration.

Measurements of length changes

An electromagnetic puller of the type described previously (Edman and Reggiani, 1984) was used for performing controlled length changes of the muscle fibers. The technique used for recording changes in length of a marked segment of the fiber was the same as that described by Edman and

Lou (1990). Two opaque markers cut from letterpress (approximately 75 μm×75 μm; mass approximately 0.1 μg) were attached to the upper surface of the fiber with the non-glue side of the letterpress material facing downwards, the distance between the markers being 0.3–0.35 mm. A laser beam, expanded to cover the marked segment, illuminated the fiber from below, and a magnified image of the segment was projected onto a photodiode array (Fairchild CCD 133, Milpitas, CA, USA). The distance between the two markers was read throughout a contraction with a time resolution of 40 μs. An analogue circuit converted the output from the photodiode array to a signal proportional to the percentage change of the segment length. The accuracy of the measurement was better than 0.2% of the segment's length.

The marker recording technique was used in certain experiments for actively controlling the length of the segment during the stimulation period ('segment length clamp'). This was achieved by adjusting the overall length of the fiber appropriately using the segment-length signal for feedback control of the electromagnetic puller. Using this approach, it was possible to make the segment shorten at a given speed to a predetermined sarcomere length, to be held stationary at this length for the remainder of the activity period. This was accomplished by altering the reference level of the feedback system by means of a voltage ramp. A small initial transient of the length signal, covering approximately 5 ms, frequently occurred affecting the onset of tension rise during the corresponding time.

Load-clamp recording

Load clamping for isotonic shortening was carried out by rapidly changing the mode of operation of the electromagnetic puller from fiber-length control to force control. The switch-over to force control occurred during the plateau of a 1-s tetanus (approximately 400–500 ms after the onset of stimulation), and the force-control mode was thereafter maintained throughout the tetanus period. With the experimental device used it was possible to achieve a period of stable tension over a wide force range, even quite close to zero force level. In the present series of experiments, the load was varied between P_0 (isometric force) and $\leqslant$5% P_0 (five experiments), and between P_0 and 8% P_0 (one experiment).

Recording and measurement of data

The signals of the force and displacement transducers, and the segment-length signal were fed into an acquisition and analysis program (Labview, National Instruments, Austin, TX, USA) and stored on disks. For the analysis of the force–velocity relationship, the slope of the digital length records was measured within the relatively straight portion of the record that occurred after the initial transient had been passed during the force-clamp manoeuvre. The slope was measured over a time interval of approximately 20 ms using a computer program based on the least-squares method.

The force–velocity relation was biphasic with two distinct curvatures on either side of a breakpoint near 80% of the measured isometric force, similar to the situation in extra- and intrafusal fibers of frog muscle (Edman, 1988; Edman et al., 2002). The biphasic equation previously described (Edman, 1988) was used to fit the experimental data:

$$V = \frac{(P_0^* - P)\mathrm{b}}{P + \mathrm{a}} \left(1 - \frac{1}{1 + e^{-\mathrm{k}_1(P - \mathrm{k}_2 P_0)}} \right), \qquad (1)$$

where V is the velocity of shortening, P the load on the muscle fiber and P_0 the measured isometric force. The first term of the equation expresses the force–velocity relation below 0.8 P_0, and represents a rectangular hyperbola in the form described by Hill (1938). P_0* is the isometric force predicted from this hyperbola, and a and b are constants with dimensions of force and velocity, respectively. The second term within parenthesis [referred to as the 'correction term' (Edman, 1988)] reduced V at high loads to fit the distinct upward-concave curvature at loads greater than approximately 0.8 P_0. The constant k_1 in the correction term has the dimension of 1/force, whereas k_2 is dimensionless. k_1 determines the steepness of the high-force curvature and k_2 the relative force at which the correction term reaches its half value. The two constants are useful parameters when comparing data from different studies.

Statistics

All statistics are given as means ± S.E.M. Student's *t*-test was used for determination of statistical significance.

Results

Time course of the isometric tetanus

Fig. 1A illustrates an isometric (fixed-fiber ends) recording of a fused tetanus in an isolated mouse muscle fiber at optimal length, and Fig. 1B shows the development of tetanic force in the same fiber as a short (~0.3 mm) segment was held at constant length during the activity period. The rising phase of the isometric tetanus (Fig. 1A) was relatively slow, with approximately 300 ms being required to reach a constant level. The time for reaching 90% of maximum tetanic force during standard isometric recording was 202±20 ms in 17 single mouse fibers (21–27°C). This is to be compared with 59±4 ms (N=20) recorded in a parallel study in this laboratory on frog skeletal muscle fibers (*Rana temporaria*) at 20–22°C (pH 7.0, intervals between tetani: 3 min; K. A. P. Edman and T. Radzyukevich, unpublished).

The maximum tetanic force determined in 10 different mouse fibers was 368±57 kN m^{-2} (21–27°C). For comparison, a mean tetanic force of 416±16 kN m^{-2} (N=20) was recorded in the frog single muscle fibers at optimal length at 20–22°C (K. A. P. Edman and T. Radzyukevich, unpublished). The tetanic force produced by the mouse fibers was thus not significantly different from that generated by *Rana temporaria* muscle fibers at 21°C. It is of interest to note that substantially lower mean values of the isometric tetanic force (291 and 258 kN m^{-2}) have been recorded in the high temperature range

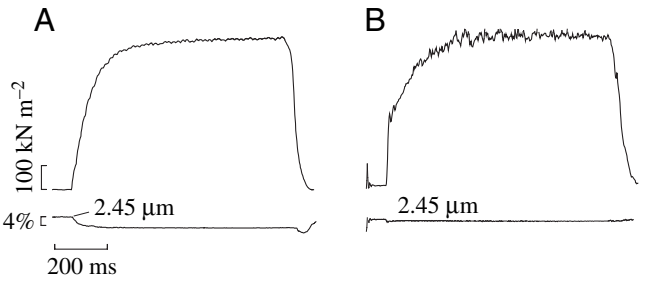

Fig. 1. Example records of fused isometric tetanus of an isolated muscle fiber of the mouse. (A) Standard 'isometric' recording (fixed fiber ends). (B) Force production during length clamp of a fiber segment. Upper trace in each panel shows force; lower trace, segment length recording with sarcomere spacing indicated. A downward deflexion of segment length signal indicates shortening. An initial transient at the onset of the length-clamp manoeuvre in B caused the early tension step. Note, however, that the time required to reach plateau force is quite similar during contraction with fixed fiber ends and during segment length-clamp recording. The intrinsic shortening during the standard isometric recording in A was 5.0% of fibre length. Temperature, 23.5°C.

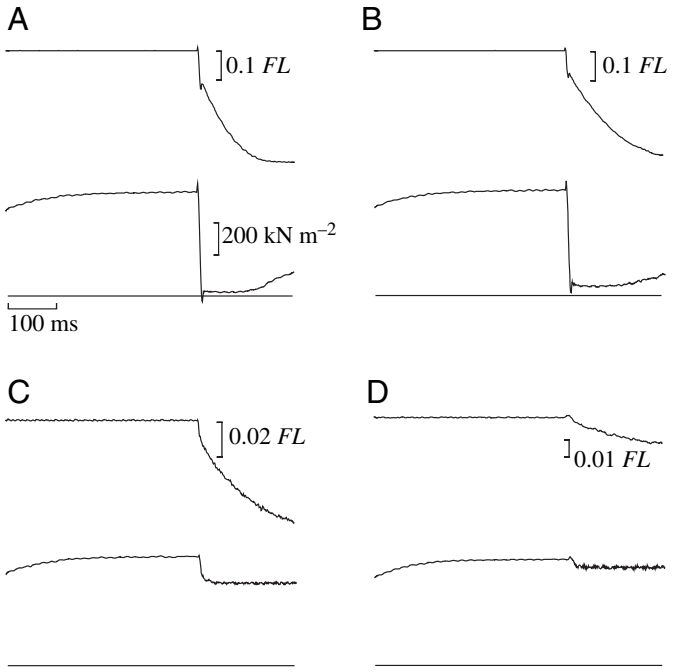

Fig. 2. Load-clamp recordings at four different force levels during tetanus of a mouse single muscle fiber. (A–D) In each set of records traces represent (from the top): fiber length (puller signal), tetanic force and base line of force. Calibrations of time and force are the same in A–D. A downward deflection of puller signal (*FL* = fiber length) denotes shortening. Note the different calibrations of puller signal in A–D. The resting fiber length was 0.58 mm. Temperature, 23.5°C.

(20–24°C) by Cecchi et al. (1978) and Piazzesi et al. (2003), in studies of single fibers from *Rana esculenta*.

The possibility was considered that the slow onset of tetanic force might be due to a larger series compliance within the mammalian fiber during activity, as this would delay the attainment of steady force. In order to test this point, experiments were performed in which a short (~0.3 mm) segment, located midway between the tendons, was held at constant length during stimulation (see Materials and methods). As illustrated in Fig. 1B, the rate of rise of force during length-clamp recording (following the initial transient at the onset of activation; see Materials and methods) was quite similar to that recorded under standard conditions, suggesting that the slow attainment of maximum force reflects a lower rate of activation of the mammalian fibers.

Force–velocity relationship

Load-clamp recordings at different loads performed in a mouse single muscle fiber are illustrated in Fig. 2. As can be seen, constant force could be attained within 15–25 ms of switching from length- to force-control of the electromagnetic puller. The slope of the length records was determined by regression analysis within a time interval of approximately 20 ms after the initial transient had been passed during the load-clamp manoeuvre (see Materials and methods). Fig. 3 illustrates a typical force–velocity analysis with data points ranging from P_0 (isometric force) to 3% P_0. The force–velocity relationship of the mouse muscle fibers exhibited the same characteristic biphasic shape as has been previously demonstrated in frog muscle fibers (Edman, 1988). The force–velocity relationship can thus be seen to have two distinct curvatures located on either side of a breakpoint near 80% of the isometric force. The two phases of the force–velocity relationship, and the location of the breakpoint, are most clearly illustrated in the semilogarithmic plot shown in Fig. 3B. The data displayed in the standard forcevelocity diagram (Fig. 3A) can be fitted well by the biphasic equation (see Eqn 1) that has previously been employed to characterize the force–velocity relationship in frog muscle fibers (Edman, 1988). In this equation, the constant k_1 expresses the degree of curvature at high loads, whereas k_2 indicates the position of the high-force curvature along the force axis (see Materials and methods).

Numerical values of the various parameters in Eqn 1 derived from six different experiments are summarised in Table 1. The data are in general agreement with those obtained in frog muscle fibers. The extension of the curve derived at low and intermediate loads can be seen to intersect the abscissa at a point, P_0*, that was considerably (mean, 1.4×) higher than the measured isometric force P_0, indicating that the power output of the fiber decreased dramatically as the load exceeded the breakpoint of the force–velocity relation.

V_{max}, the speed of shortening at zero load estimated from the force–velocity curve, was 4.0±0.3 L s^{-1} (N=6, 23.1–23.8°C). A higher value of the maximum speed of shortening (7.89± 0.35 L s^{-1}, 22–24°C) of intact fibers from the same muscle species (mouse, NMRI) has been reported by Westerblad et al. (1998), using the slack-test method (Edman, 1979). This difference in results is not readily understood but could mean

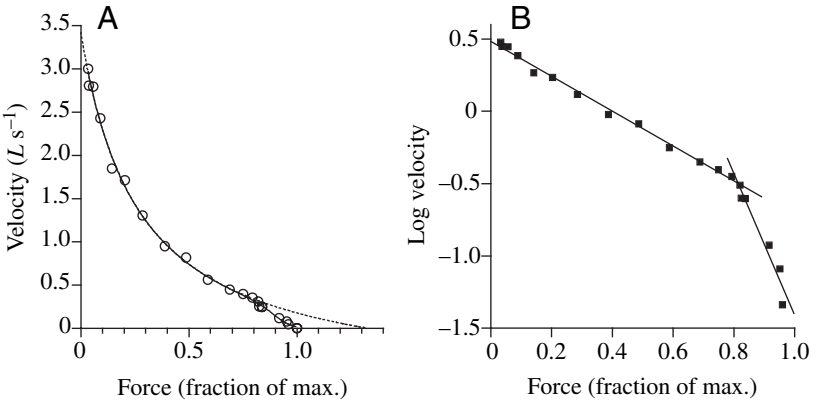

Fig. 3. Biphasic force–velocity relationship. Force–velocity data collected from a mouse isolated muscle fiber are illustrated in a conventional diagram in (A) and as a semilogarithmic plot in (B). Data in A fitted by Eqn 1 (see Materials and methods) using the following numerical values for constants: k_1=24.08 P_0^{-1}; k_2=0.85; a/P_0*=0.27. Dashed line in A indicates a continuation of the hyperbola derived at low and intermediate loads. The straight lines in B are linear regressions of shortening velocity upon force on either side of the breakpoint of the force–velocity relationship. Note the distinct breakpoint of the force–velocity relationship near 0.8 P_0. Temperature, 23.5°C.

that the measurements in the two studies refer to different portions of the multi-headed muscle. It should be pointed out that hyperbolic extrapolation of force–velocity data derived at finite loads may provide a somewhat lower value of the maximum shortening velocity than that derived by a slack-test analysis (for details, see Edman, 1979; Josephson and Edman, 1988). However, as the present study included load-clamp measurements quite close to zero load, it is reasonable to conclude that the value of V_{max} derived in the present study does represent a valid estimate of the maximum speed of shortening in the fibers used (see Josephson and Edman, 1988). Considerably higher speeds of shortening than those produced by the mouse fibers were recorded in frog single muscle fibers at the same temperature (19.3–22.7°C) in this laboratory (K. A. P. Edman and T. Radzyukevich, unpublished). The speed of unloaded shortening (slack tests) of the frog fibers was found to be 8.2±1.9 L s^{-1} (N=19), i.e. twice the value derived in the present study of mouse muscle fibers.

Length–tension relationship

A series of experiments was performed in which the tetanic force of a marked, length-clamped segment (approximately 0.3 mm in length) of a single mouse muscle fiber was recorded at different sarcomere lengths. The sarcomere length was determined by measuring the space taken up by rows of 20 sarcomeres using a microscope at 800× magnification as described in Materials and methods. This measurement was carried out with the fiber adjusted to just above slack length. Before starting the sarcomere length measurement, the fiber was stretched passively 2–3 times to an extreme length. The sarcomere spacing during activity was calculated from the measured sarcomere length at rest and the overall change in length of the marked segment. The force measurements during length-clamp recording were performed in repeated sequences in both directions along the descending limb of the length-tension relation. Force measurements below slack length were performed during standard isometric recording (fixed fiber ends), as tension creep was insignificant during the tetanus under these conditions (see below).

Fig. 4A illustrates length-clamp recordings during tetanic stimulation at sarcomere lengths within the plateau region and the descending limb of the length-tension relation, and Fig. 4B shows standard isometric tetani recorded on the ascending limb of the length-tension relation. In both cases, the force records can be seen to exhibit a minimum of tension creep, and they may therefore be considered to represent the actual capacity of the fiber to produce force at the various sarcomere lengths.

Fig. 5 illustrates the variation in force, with sarcomere length based on data compiled from three mouse fibers (one for the ascending limb and three for the descending limb), the data points being normalised to the force recorded at 2.45 μm sarcomere length in the respective fiber. The straight line is the linear regression of force upon sarcomere length calculated for values between 2.35 μm and 4.0 μm (correlation coefficient: 0.96). The line intersects the abscissa at 3.88 μm and reaches maximum force (1.0) at 2.40 μm. The latter value thus represents the calculated right end of the plateau of the length-tension relation, i.e. the point where, theoretically, the thin filaments have reached the inert, or bare, zone in the middle of the thick filaments. Based on this assumption, the regression line in Fig. 5 suggests that the average length of the actin filaments is 1.10 μm. For this calculation, it is assumed that the bare zone of the thick filament is 0.16 μm (Craig and Offer, 1976; ter Keurs et al., 1984) and the width of the Z disk is 0.05 μm (Page and Huxley, 1963). On the same assumptions, the intersection of the regression line with the abscissa at 3.88 μm sarcomere length is compatible with an average thick filament length of 1.63 μm. The values of the thick and thin filament lengths so derived agree exceedingly well with recent electron microscopical measurements of the two filaments in rabbit psoas muscle (Sosa et al., 1994).

Tetanic force stays fairly constant between 2.1 and 2.4 μm sarcomere length and can be seen to decrease steeply by reducing the sarcomere length below 2.0 μm; at 1.5 μm

Table 1. *Parameters of the force–velocity relation calculated according to Equation 1*

k_1	21.45±1.22 P_0^{-1}
k_2	0.85±0.004
a/P_0	0.20±0.02
P_0*	1.40±0.08 P_0
V_{max}	4.0±0.3 L/s

Values are means ± S.E.M., N=6.

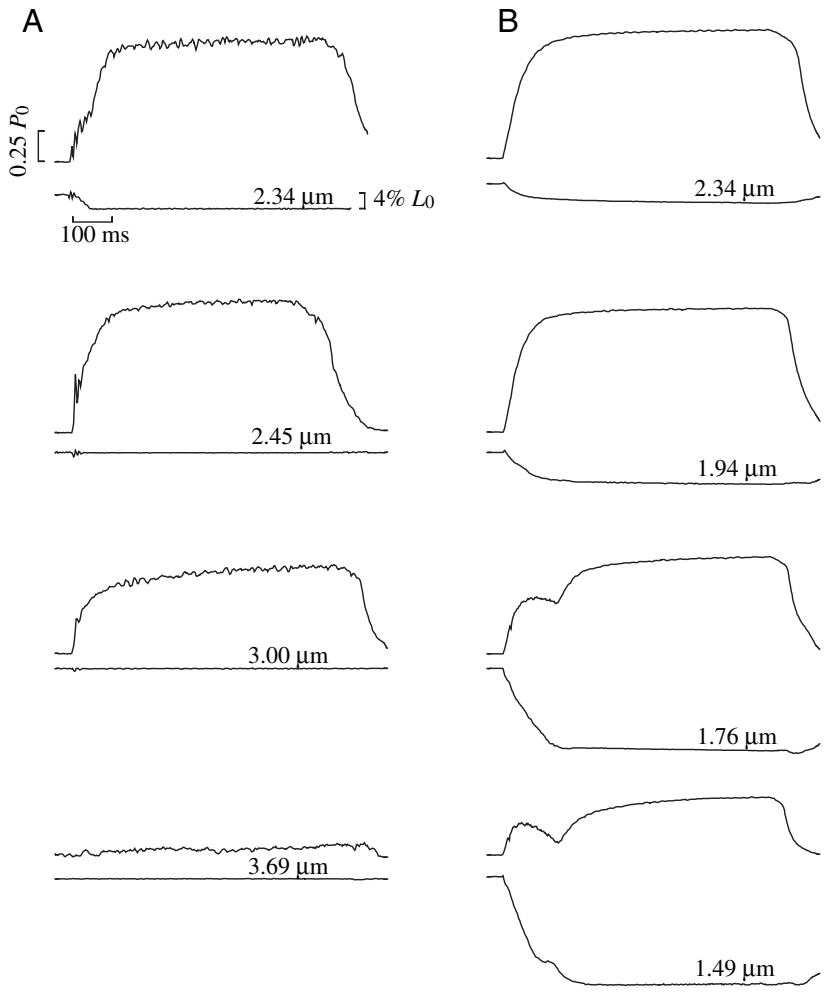

Fig. 4. Records of tetanic contractions in a single muscle fiber at optimum sarcomere length and along the descending (A) and ascending (B) limbs of the length–tension relationship. Records shown in A were derived by holding a discrete fiber segment at a constant length during the tetanus. For records below the slack length, the segment was initially shortened under segment length control to the desired sarcomere spacing. Records in B are standard isometric contractions (no segment-length control) of the same fiber as in A. For contractions at moderately reduced lengths, the fiber was allowed to shorten freely to the desired length by taking up a pre-set slack. For contractions below approximately 1.9 μm, the initial shortening phase was constrained by applying a controlled ramp movement of the electromagnetic puller. The latter manoeuvre made the fiber develop some tension during the initial shortening phase. The upper trace in each set of records shows force; the lower trace shows segment length recording with sarcomere spacing indicated. A downward deflexion of segment length signal indicates shortening. P_0, measured isometric force at 2.45 μm sarcomere length; L_0, segment length at 2.45 μm sarcomere length. Temperature, 24.1°C.

sarcomere spacing, the measured force was merely 45% of the plateau value.

The asterisks plotted along the ascending limb of the length-tension relation (Fig. 5) are estimated values of force based on the model previously described in a corresponding study of frog muscle fibres (Edman and Reggiani, 1987). The following assumptions were used: (1) active force is produced in proportion to the amount of single overlap (O_S, inset, Fig. 5) between adjacent thick and thin filaments; (2) the decrease in tension below optimum length is attributed to the occurrence of double filament overlap (O_D, inset, Fig. 5) that leads to a decrease in the number of active cross-bridges or, alternatively, to a force opposing filament sliding; and (3) an additional counteracting force is thought to arise as the ends of the thick filaments are compressed as a result of collision with the Z disks at lengths below 1.68 μm sarcomere length. The expected force along the ascending limb of the length-tension relation was thus derived from the following expression:

$$F = O_S K_S - O_D K_D - O_C K_C , \qquad (2)$$

where K_S, K_D and K_C are proportionality coefficients with dimensions of force per micrometer filament overlap per half sarcomere. For these calculations, the above numerical values of the filament lengths, the widths of the *Z* disk and the bare zone have been used, and the calculated force (F) is expressed in units of the force calculated at optimum sarcomere length, i.e. at 2.40 μm sarcomere length, where O_S (=0.735 μm) is maximum (see above). The numerical value of K_S used for calculating the force was therefore the reciprocal of 0.735.

Fig. 5 (asterisks) shows the predicted force at selected sarcomere lengths calculated according to the above model, assuming that the three proportionality coefficients have the same numerical value, 1/0.735. As can be seen, the predicted force values accord remarkably well with the actual measurements of force below optimal length.

Discussion

With the experimental approach used it has been possible to study the contractile properties of intact single mammalian muscle fibers with a precision comparable to that reached in previous studies on frog muscle fibers. The isolated preparations, approximately 0.5 mm in length and 25–40 μm wide, gave stable responses over many hours of experimentation, and measurements of force and movement were achieved both from the fiber as a whole and, in certain experiments, from a marked segment whose length was controlled by a servo system. Some pertinent similarities and differences in the mechanical behaviour with respect to previous observations in amphibian muscle fibers are considered here.

Time course of mechanical activation

The onset of tension rise during tetanic stimulation was

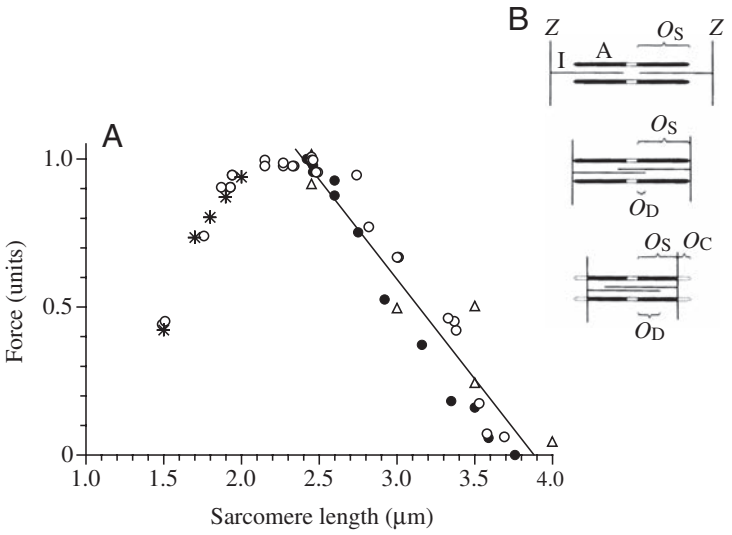

Fig. 5. Tetanic force *versus* sarcomere length recorded in mouse single muscle fibers. (A) Force expressed in units of the tetanic force recorded near 2.4 μm sarcomere length. The straight line is linear regression of force upon sarcomere length for values between 2.35 and 4.00 μm sarcomere length. Asterisks along the ascending limb are calculated force values based on the assumptions described in text. (B) Schematic illustration of different degrees of overlap between thick (A) and thin (I) filaments. O_S, single filament overlap; O_D, double filament overlap; O_C, compression of thick filaments when colliding with *Z* disks at short (<1.7 μm) sarcomere lengths. Reproduced, with permission, from Edman and Reggiani (1987). For further information, see text.

found to be less steep in the mouse fibers than in frog muscle fibers, the time required to reach 90% of maximum force being approximately four times longer in the mammalian fibers when measured at equal temperatures (20–25°C). The possibility was ruled out that the relatively slow rise of the tetanic force during standard isometric recording (fixed fiber ends) was due to larger series compliance in the mammalian preparation, which would delay the attainment of maximum force. This was achieved by recording force while a short (approximately 0.3 mm) segment was held at constant length during tetanic stimulation, in this way eliminating any influence on the force measurement by compliant structures outside the domain of the fiber segment. The length-clamp recording confirmed the relatively slow development of force observed during standard recording, indicating that this is a characteristic feature of the mammalian fiber at sarcomere level.

Force–velocity relationship

The results show that the force–velocity relationship of the mouse muscle fibers has the same biphasic shape as has been previously demonstrated in frog muscle (Edman, 1988; Edman et al., 1997), i.e. there are two distinct curvatures, both with an upwards concave shape, on either side of a breakpoint near 80% of the isometric force. The force–velocity data could be fitted well with the biphasic equation that has previously been applied to frog muscle fibers, using quite similar numerical values of the parameters defining the two curvatures of the force–velocity relationship.

The present results strengthen the view that the biphasic shape of the force–velocity relation is a genuine property of the contractile system in striated muscle, and its relevance in muscle function is twofold. (1) By this arrangement the muscle is capable of producing a relatively high-power output at intermediate loads, the region most often used during muscle work. (2) At the same time, because of the sharp decrease in velocity at loads exceeding 80% of P_0, the muscle has acquired a mechanism designed to stabilize the myofilament system at high loads.

As has been previously demonstrated in frog muscle fibers (Edman, 1988), there is a smooth continuation of the force–velocity relation as the load exceeds P_0, and the muscle fiber is being stretched, resulting in a flat sigmoidal force–velocity relationship with inflexion at P_0. This feature of the force–velocity relationship implies that there is a fairly wide region around P_0 (cf. fig. 7 in Edman, 1988) where the force may be allowed to vary substantially with little change in speed of shortening or lengthening. This provides an expedient mechanism of stabilizing the myofilament system, in that stronger and weaker regions in series will stay nearly isometric in the high-load range, i.e. any tendency towards redistribution of sarcomere length between weaker and stronger segments will be minimized.

The molecular mechanism underlying the high-force curvature of the force–velocity relationship dealt with in the present paper is still incompletely understood, but all the evidence would seem to suggest that the biphasic shape of the force–velocity curve is an inherent feature of the sliding filament process. Supporting this view, the high-force deviation of the force–velocity relation appears in skinned muscle fibers, as well as in intact preparations, and is unrelated to the state of activation of the contractile system (Lou and Sun, 1993; Edman et al., 1997). Several attempts have been made to simulate the characteristic change of the force–velocity relation in the high-force range (0.8 P_0–P_0) based on different cross-bridge models (Mitsui and Chiba, 1996; Edman et al., 1997; Nielsen, 2003). The cross-bridge model presented by Edman et al. (1997) was found to simulate the experimental force–velocity and stiffness–velocity relationships exceedingly well. An important aspect of this model is the assumption of a Gaussean position-dependence of the attachment rate constant along the thin filament, in this way creating a region early during the power stroke where the cross-bridge attachment is slow. This feature of the model leads to a marked decrease in the number of pulling cross-bridges during shortening in the high-force range, and to a lower force output per bridge. Together, these changes account for the upwards-concave region of the force–velocity relation at high loads (0.8 P_0–P_0) according to the model.

The length-tension relationship

The length-tension relationship in mammalian muscle has

previously been delineated in studies of skinned fibers (Stephenson and Williams, 1982) and intact muscle fiber bundles (ter Keurs et al., 1984) from rat skeletal muscle. The present study is a first attempt to determine this relationship in intact single fibers from a mammalian muscle. With the technique used, it was possible to measure tetanic force without appreciable tension creep from a short marked segment along the fiber by holding the selected segment at constant length throughout the stimulation period by feedback control. The results show that the tetanic force stays quite constant within a range of sarcomere lengths, from approximately 2.1 to 2.4 μm, from which point the force starts to decline linearly with further extension of the sarcomeres. A considerably wider plateau region (extending from approximately 2.1 to 2.7 μm sarcomere length) was derived by Stephenson and Williams (1982) and ter Keurs et al. (1984). This difference in results is explainable by assuming that there was a wider dispersion of sarcomere length in the earlier experiments.

The slope of the descending limb of the length-tension relation provides relevant information on the effective lengths of the myofilaments. As described in the Results, the linear regression of the data points along the descending limb is consistent with an average thin-filament length of 1.10 μm and an average thick filament length of 1.63 μm, both values according well with recent electron microscope measurements in mammalian muscles (Sosa et al., 1994).

The above values of the thick and thin filaments also accord with the slope of the ascending limb of the length-tension relation, if it is assumed that active force is reduced in proportion to the length of double filament overlap (O_D) and the amount of compression of the thick filaments (O_C) when colliding with the Z disk. The good agreement between the calculated and experimental data shown in Fig. 5 is based on the assumption that the proportionality coefficients K_D and K_C have the same numerical value as that of K_S (see Results). This is in line with the idea that the thin filaments intruding from the opposite half of the sarcomere prevent any interaction between the thick and thin filaments within the region of double filament overlap.

The present observation differs from the results obtained in a similar study on frog muscle fibers (Edman and Reggiani, 1987) in that the proportionality coefficient K_D required a value 1.7× larger than that of K_S in order to fit the frog muscle data. The ascending limb of the length-tension relation in frog muscle fibers is thus steeper than predicted on the basis of filament overlap as discussed above. The relatively steep decline of tension below optimal length in frog muscle fibers is also apparent in the earlier studies by Gordon et al. (1966) and Edman (1966) (see fig. 9 in Edman and Reggiani, 1987).

The mechanism underlying the greater steepness of the ascending limb in frog muscle fibers is still unclear. A possibility worth considering would be that the relatively wide frog muscle fibers become incompletely activated during tetanic stimulation at short lengths because of decremental inward spread of activation as the fiber diameter expands with shortening (Taylor and Rüdel, 1970; however, see Gonzalez-Serratos, 1975). This would reduce the force output below the expected values along the ascending limb in the frog fibers. Failure of the inward spread of activation is, however, unlikely to affect the mechanical output of the much thinner mammalian fibers used in the present study.

This work was supported by grants from the Swedish Medical Research Council (projects 14X-184 and 14X-08664) and from the Royal Physiographical Society. I wish to thank Britta Kronborg for her excellent technical assistance. Thanks are also due to Professor A. Arner for kindly providing office and laboratory facilities.

References

Blinks, J. R. (1965). Influence of osmotic strength on cross-section and volume of isolated single muscle fibres. *J. Physiol*. **177**, 42-57.

Cecchi, G., Colomo, F. and Lombardi, V. (1978). Force-velocity relation in normal and nitrate-treated frog single muscle fibers during rise of tension in an isometric tetanus. *J. Physiol.* **285**, 257-273.

Craig, R. and Offer, G. (1976). Axial arrangement of crossbridges in thick filaments of vertebrate striated muscle. *J. Mol. Biol.* **102**, 325-332.

Edman, K. A. P. (1966). The relation between sarcomere length and active tension in isolated semitendinosus fibers of the frog. *J. Physiol.* **183**, 407-417.

Edman, K. A. P. (1979). The velocity of unloaded shortening and its relation to sarcomere length and isometric force in vertebrate muscle fibers. *J. Physiol.* **291**, 143-159.

Edman, K. A. P. (1988). Double-hyperbolic force-velocity relation in frog muscle fibers. *J. Physiol.* **404**, 301-321.

Edman, K. A. P. and Reggiani, C. (1984). Redistribution of sarcomere length during isometric contraction of frog muscle fibers and its relation to tension creep. *J. Physiol.* **351**, 169-198.

Edman, K. A. P. and Reggiani, C. (1987). The sarcomere length-tension relation determined in short segments of intact muscle fibers of the frog. *J. Physiol.* **385**, 709-732.

Edman, K. A. P. and Lou, F. (1990). Changes in force and stiffness induced by fatigue and intracellular acidification in frog muscle fibers. *J. Physiol.* **424**, 133-149.

Edman, K. A. P. and Lou, F. (1992). Myofibrillar fatigue *versus* failure of activation during repetitive stimulation of frog muscle fibers. *J. Physiol.* **457**, 655-673.

Edman, K. A. P., Månsson, A. and Caputo, C. (1997). The biphasic force-velocity relationship in frog muscle fibers and its evaluation in terms of cross-bridge function. *J. Physiol.* **503**, 141-156.

Edman, K. A. P., Radzyukevich, T. and Kronborg, B. (2002). Contractile properties of isolated muscle spindles of the frog. *J. Physiol.* **541**, 905-916.

Ford, L. E., Huxley, A. F. and Simmons R. M. (1977). Tension responses to sudden length change in stimulated frog muscle fibers near slack length. *J. Physiol.* **269**, 441-515.

González, E., Messi, M. L., Zheng, Z. and Delbono, O. (2003). Insulin-like growth factor-1 prevents age-related decrease in specific force and intracellular Ca^{2+} in single intact muscle fibres from transgenic mice. *J. Physiol.* **552**, 833-844.

Gonzalez-Serratos, H. (1975). Graded activation of myofibrils and the effect of diameter on tension development during contractures in isolated skeletal muscle fibers. *J. Physiol.* **253**, 321-339.

Gordon, A. M., Huxley, A. F. and Julian, F. J. (1966). The variation in isometric tension with sarcomere length in vertebrate muscle fibers. *J. Physiol.* **184**, 170-192.

Hill, A. V. (1938). The heat of shortening and the dynamic constants of muscle. *Proc. R. Soc. London, Ser. B* **126**, 136-195.

Josephson, R. K. and Edman, K. A. P. (1988). The consequences of fiber heterogeneity on the force-velocity relation of skeletal muscle. *Acta Physiol. Scand.* **132**, 341-352.

Lou, F. and Sun, Y.-B. (1993). The high-force region of the force-velocity relation in frog skinned muscle fibers. *Acta Physiol. Scand.* **148**, 243-252.

Mitsui, T. and Chiba, H. (1996). Proposed modification of the Huxley-

Simmons model for myosin head motion along an actin filament. *J. Theor. Biol.* **182**, 147-159.

Nielsen, B. G. (2003). Unfolding transitions in myosin give rise to the double-hyperbolic force-velocity relation in muscle. *J. Phys. Condens Matter* **15**, S1759-S1765.

Page, S. and Huxley, H. E. (1963). Filament lengths in striated muscle. *J. Cell Biol.* **19**, 369-390.

Piazzesi, G., Lucii, L. and Lombardi, V. (2002). The size and the speed of the working stroke of muscle myosin and its dependence on the force. *J. Physiol.* **545**, 145-151.

Piazzesi, G., Reconditi, M., Koubassova, N., Decostre, V., Linari, M., Lucii, L. and Lombardi, V. (2003). Temperature dependence of the force-generating process in single fibers from frog skeletal muscle. *J. Physiol.* **549**, 93-106.

Sosa, H., Popp, D., Ouyang, G. and Huxley, H. E. (1994). Ultrastructure of skeletal muscle fibers studied by a plunge quick freezing method: myofilament lengths. *Biophys. J.* **67**, 283-292.

Stephenson, D. G. and Williams, D. A. (1982). Effects of sarcomere length on the force-pCa relation in fast – and slow-twitch skinned muscle fibers from rat. *J. Physiol.* **333**, 637-653.

Taylor, S. R. and Rüdel, R. (1970). Striated muscle fibers: inactivation of contraction induced by shortening. *Science* **167**, 882-884.

Ter Keurs, H. E., Luff, A. R. and Luff, S. E. (1984). Force-sarcomere-length relation and filament length in rat extensor digitorum muscle. *Adv. Exp. Med. Biol.* **170**, 511-525.

Westerblad, H., Dahlstedt, A. J. and Lännergren, J. (1998). Mechanisms underlying reduced maximum shortening velocity during fatigue of intact, single fibers of mouse muscle. *J. Physiol.* **510**, 269-277.